



## $^{26}\text{Al}$ and $^{60}\text{Fe}$ yields from AGB stars

Maria Lugaro<sup>a,b,\*,1</sup>, Amanda I. Karakas<sup>c,2</sup>

<sup>a</sup> Sterrekundig Instituut, Universiteit Utrecht, P.O. Box 80000, 3508 TA Utrecht, The Netherlands

<sup>b</sup> Centre for Stellar and Planetary Astrophysics, School of Mathematical Sciences, Monash University, Victoria 3800, Australia

<sup>c</sup> Research School of Astronomy and Astrophysics, Mt. Stromlo Observatory, Cotter Road, Weston, ACT 2611, Australia

### ARTICLE INFO

#### Article history:

Available online 2 July 2008

#### PACS:

26.20.Np

#### Keywords:

Stars: AGB

Post-AGB

Nucleosynthesis

Abundances

### ABSTRACT

We present yields for  $^{26}\text{Al}$  and  $^{60}\text{Fe}$  from asymptotic giant branch (AGB) stars. For AGB stars of masses lower than  $\approx 4 M_{\odot}$ , yields are of the order of only  $10^{-7} M_{\odot}$ , while for AGB stars of higher masses yields are up to  $10^{-5} M_{\odot}$ . In these massive AGB stars  $^{26}\text{Al}$  is produced via  $^{25}\text{Mg}(p,\gamma)^{26}\text{Al}$  reactions when proton captures occur at the base of the convective envelope (hot bottom burning), while  $^{60}\text{Fe}$  is produced via the operation of the  $^{59}\text{Fe}(n,\gamma)^{60}\text{Fe}$  reaction when high neutron densities result from the activation of the  $^{22}\text{Ne}(\alpha,n)^{25}\text{Mg}$  neutron source during thermal pulses. Large nuclear and stellar uncertainties are associated with these predictions, ranging from the rate of the  $^{26}\text{Al} + p$  reaction to the amount of material carried from the He-rich shell to the convective envelope via the third dredge-up. When compared to the contribution from core-collapse supernovae, the overall contribution of AGB stars to the Galactic inventory of  $^{26}\text{Al}$  and  $^{60}\text{Fe}$  is insignificant. On the other hand, a massive AGB star may have polluted the early solar system with short lived radioactive nuclei since we obtain a self-consistent match for the abundances of  $^{41}\text{Ca}$ ,  $^{26}\text{Al}$ ,  $^{60}\text{Fe}$ , and  $^{107}\text{Pd}$  using our  $6.5 M_{\odot}$  model. Finally, the interpretation of the  $^{26}\text{Al}/^{27}\text{Al}$  ratios in the majority of meteoritic stellar grains from low-mass AGB stars is hindered by the three orders of magnitude error bar of the  $^{26}\text{Al}(p,\gamma)^{27}\text{Si}$  reaction. Grains with very high  $^{26}\text{Al}/^{27}\text{Al}$  ratios may represent evidence for extra-mixing phenomena in AGB stars or for a post-AGB origin.

© 2008 Elsevier B.V. All rights reserved.

### 1. The evolution of AGB stars and the production of radioactive nuclei

The asymptotic giant branch (AGB) is the final nuclear-burning phase of stars with initial masses less than  $\approx 7 M_{\odot}$ . AGB stars are composed of an inert C–O core surrounded by an inner He-burning shell, an intershell rich in He and carbon, and an outer H-burning shell. On top of this double shell configuration sits a large convective envelope, where most of the stellar mass resides. Material at the surface is constantly eroded by stellar winds, which greatly increase their strength with time eventually leading to the complete ejection of the envelope, the formation of a planetary nebula, and the evolution of the former stellar degenerate C–O core into a cooling white dwarf. During the AGB phase, the H and He-burning shells are activated alternately in the deep layers of the star. The H-burning shell is the main energy source for most of the AGB evolution, however, the thinness of the He-shell along with a slight

degeneracy means that once the overlying layers compress and heat, a thermal instability or runaway takes place. These thermal pulses (TPs) trigger convection in the whole intershell, which acts to homogenise abundances within that region. After a thermal pulse is quenched, the base of the convective envelope can sink into the intershell (third dredge-up, TDU), carrying to the surface nuclear processed material (see Herwig, 2005 for a review on AGB stars).

In the intershell of AGB stars  $^{12}\text{C}$ ,  $^{19}\text{F}$ ,  $^{22}\text{Ne}$ , and the heavy Mg isotopes are produced by partial He burning in thermal pulses. Free neutrons are released by the  $^{13}\text{C}(\alpha,n)^{16}\text{O}$  reaction during the interpulse periods and by the  $^{22}\text{Ne}(\alpha,n)^{25}\text{Mg}$  reaction during TPs, leading to the production of elements heavier than Fe via *slow* neutron captures (the *s* process). The  $^{13}\text{C}$  neutron source produces neutron densities up to  $\approx 10^8 \text{ n/cm}^3$  and a large integrated neutron flux. The neutrons are released in a small radiative region ( $< 10^{-4} M_{\odot}$ ) of the He intershell. Protons from the envelope are assumed to have diffused downwards into the intershell at the end of each TDU episode and be captured by the abundant  $^{12}\text{C}$  to make  $^{13}\text{C}$ . The  $^{13}\text{C}$  neutron flux leads to the production of the main component of the *s* process, i.e.  $90 < A < 206$ , in AGB stars of masses between  $1.5 M_{\odot}$  and  $3 M_{\odot}$  (Gallino, 1998). Along the main *s*-process path several radioactive nuclei are present:  $^{93}\text{Zr}$ ,  $^{99}\text{Tc}$ ,  $^{107}\text{Pd}$ , and  $^{205}\text{Pb}$ , which can be made in AGB stars by the  $^{13}\text{C}$  neutron source.

\* Corresponding author. Address: Sterrekundig Instituut, Universiteit Utrecht, P.O. Box 80000, 3508 TA Utrecht, The Netherlands.

E-mail addresses: [m.a.lugaro@uu.nl](mailto:m.a.lugaro@uu.nl) (M. Lugaro), [akarakas@mso.anu.edu.au](mailto:akarakas@mso.anu.edu.au) (A.I. Karakas).

<sup>1</sup> Supported by the Netherlands Organisation for Scientific Research (NWO).

<sup>2</sup> Supported by the Australian Research Council.

The  $^{22}\text{Ne}$  neutron source operates at temperatures greater than  $300 \times 10^6$  K and produces much higher neutron densities, up to  $\approx 10^{13}$   $n/\text{cm}^3$  along with a small integrated neutron flux. This reaction is the main neutron source in AGB stars of masses higher than  $\approx 4 M_{\odot}$ , owing to the higher peak temperatures obtained in their He-shells. The  $^{22}\text{Ne}$  neutron source is more efficient than the  $^{13}\text{C}$  neutron source in modifying the abundances of elements lighter than Fe, leading to production of relatively light radioactive nuclei such as  $^{41}\text{Ca}$ , via  $^{40}\text{Ca}(n,\gamma)^{41}\text{Ca}$ . This is because the whole convective intershell is exposed to the neutron flux. Moreover, because of the high neutron density, the  $^{22}\text{Ne}$  neutron source affects the production of nuclei that are made via branching points on the  $s$ -process path. This results in peculiar heavy-element nucleosynthesis in massive AGB stars, leading, e.g., to overproduction of the long-living radioactive isotope  $^{87}\text{Rb}$ , as observed in the luminous OH/IR stars (Garcia-Hernandez, 2007), as well as that of  $^{60}\text{Fe}$ . Nuclei made in the intershell are carried to the convective envelope via the TDU making AGB stars progressively enriched in carbon – in some case they even become carbon-rich ( $\text{C} > \text{O}$ ) – fluorine, and heavy  $s$ -process elements, such as Zr, Ba, and Pd, and radioactive nuclei like  $^{41}\text{Ca}$  and  $^{60}\text{Fe}$ .

Aluminium-26 is made by proton captures on  $^{25}\text{Mg}$ , however, most of the  $^{26}\text{Al}$  made in the H shell does not survive ingestion in the subsequent TPs where neutrons are released, given that its total neutron-capture cross section is as high as  $\approx 200$  mbarn (see also Mowlavi and Meynet, 2000). The case is different for AGB stars more massive than  $\approx 4 M_{\odot}$ : these have a large enough envelope that nucleosynthesis and energy generation due to proton captures occur at the base of the convective envelope (hot bottom burning, HBB, see, e.g., Boothroyd et al., 1994). HBB produces a high abundance of  $^{26}\text{Al}$  which is directly carried to the stellar surface by convection. Finally, because of the strong mass loss, most of the envelope is lost and  $^{26}\text{Al}$  and  $^{60}\text{Fe}$  nuclei are shed into the interstellar medium.

## 2. Results

Fig. 1 shows predictions for the yields of  $^{26}\text{Al}$  and  $^{60}\text{Fe}$  computed using the Monash nucleosynthesis code (see, e.g., Lugaro, 2004). This code takes temperatures, densities, and mixing velocities from the Mt. Stromlo Stellar Structure code (Frost and Lattanzio, 1996)

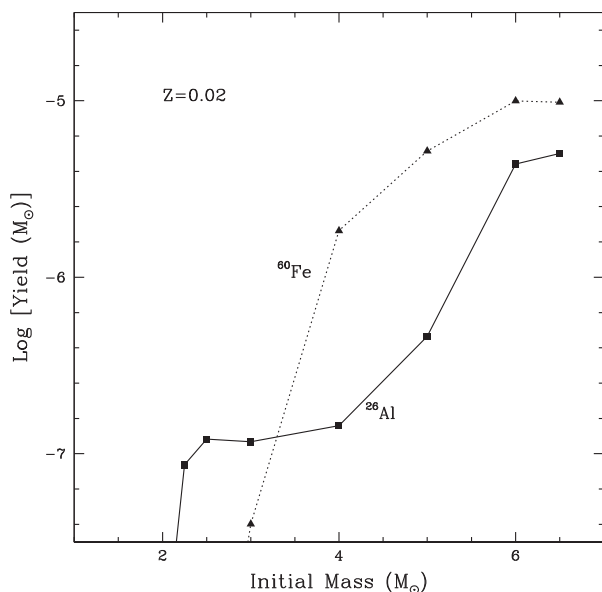


Fig. 1.  $^{26}\text{Al}$  and  $^{60}\text{Fe}$  yields from AGB models of solar metallicity and different masses (Karakas and Lattanzio, 2007).

and solves mixing and nuclear burning simultaneously following the changes in the abundances of a large number of species. We have now developed several choices of nuclear networks, the smaller from H and  $n$  to S, plus the Fe peak (77 species, 500 reactions) and the largest from H and  $n$  to S and from Fe to Pd (207 species, 1650 reactions), where missing nuclei are represented by artificial neutron sink reactions. In this way we can minimise the time needed to run the models by focusing on the isotopes we are interested in. Most of the nuclear reaction rates are from Reaclib-1991,<sup>3</sup> although we have endeavoured to update to all new available estimates when available, for example, the latest  $^{22}\text{Ne} + \alpha$  reaction rates (Karakas et al., 2006) and neutron capture cross sections from the compilation of Bao et al. (2000).

As described above, neutrons for the production of  $^{60}\text{Fe}$  are provided by the activation of the  $^{22}\text{Ne}(\alpha,n)^{25}\text{Mg}$  reaction, which depends on the temperature in the TPs. This temperature increases with the stellar mass, hence the production of  $^{60}\text{Fe}$  becomes significant for AGB stars of initial masses larger than  $3.5 M_{\odot}$ . The main uncertainties affecting the model predictions come from the neutron-capture rates of the unstable isotopes  $^{59}\text{Fe}$  and  $^{60}\text{Fe}$  itself, the error bar of the  $^{22}\text{Ne}(\alpha,n)^{25}\text{Mg}$  reaction rate, and the amount of mass carried from the intershell to the envelope by the TDU. The effect of all these uncertainties needs to be investigated in detail.

Aluminium-26 is produced (and destroyed) during HBB via the  $^{25}\text{Mg}(p,\gamma)^{26}\text{Al}(p,\gamma)^{27}\text{Si}$  reaction chain. Fig. 1 shows that a significant amount of  $^{26}\text{Al}$  is produced in AGB models of masses higher than  $5 M_{\odot}$ . Since the effect of HBB depends on the temperature achieved at the base of the convective envelope, the resulting  $^{26}\text{Al}$  yield depends on the way convection is treated. In our models we employ the mixing length theory with a parameter  $\alpha = 1.75$ . Models employing the Full Spectrum of Turbulence theory to describe envelope convection usually obtain higher temperatures at the base of the envelope (Ventura and D'Antona, 2005) which would result in a higher production of  $^{26}\text{Al}$ . Nuclear uncertainties come from the 50% error bar associated to the  $^{25}\text{Mg}(p,\gamma)^{26}\text{Al}$  reaction, and the three orders of magnitude error bar associate to the  $^{26}\text{Al}(p,\gamma)^{27}\text{Si}$  reaction. A detailed analysis of the effect of these uncertainties during HBB has been presented by Izzard et al. (2007). In particular, if the upper limit of the  $^{26}\text{Al}(p,\gamma)^{27}\text{Si}$  reaction is employed the  $^{26}\text{Al}$  production drops by two orders of magnitudes.

When compared to the results computed for massive stars exploding as core-collapse supernovae (SN) by Limongi and Chieffi (2006), AGB yields for  $^{60}\text{Fe}$  are surprisingly high: an AGB star of initial  $6 M_{\odot}$ , for example, delivers to the interstellar medium as much  $^{60}\text{Fe}$  as a SN in the mass range  $1 M_{\odot}$  to  $20 M_{\odot}$ , in spite of the fact that the initial AGB stellar mass is roughly three times smaller.  $^{26}\text{Al}$  yields from AGB stars, on the other hand, are always smaller than those from SNe by one order of magnitude. As a result, AGB stars typically produce  $^{60}\text{Fe}/^{26}\text{Al} > 1$ , while SNe typically produce  $^{60}\text{Fe}/^{26}\text{Al} < 1$ . This feature of the SN models allowed Limongi and Chieffi (2006) to produce a good match, within model uncertainties, to the  $^{60}\text{Fe}/^{26}\text{Al}$  ratio observed in Galaxy by  $\gamma$ -ray lines, for which values compatible with 0.14 have been observed. In Table 1 we show the production rates for  $^{26}\text{Al}$  and  $^{60}\text{Fe}$  computed as averages, weighted by a Salpeter initial mass function, divided by their half lives. AGB stars make an insignificant contribution to the Galactic production of  $^{26}\text{Al}$  and  $^{60}\text{Fe}$ . If AGB stars are added to the global inventory of these nuclei the  $^{60}\text{Fe}/^{26}\text{Al}$  changes from 0.117 to 0.12, preserving the match with the  $\gamma$ -ray line observations. We must point out, though, that yields for the mass range  $6.5 M_{\odot}$  to  $11 M_{\odot}$  are missing. This is the realm of super-AGB stars,

<sup>3</sup> <http://ie.lbl.gov/astro/friedel.html>.

**Table 1**  
Production rates ( $M_{\odot}/\text{Myr}$ ) of  $^{26}\text{Al}$  and  $^{60}\text{Fe}$  calculated from AGB and SN models

	AGB	SNII	AGB/SNII
$^{26}\text{Al}$	$2.7 \times 10^{-13}$	$1.1 \times 10^{-10}$	0.2%
$^{60}\text{Fe}$	$4.3 \times 10^{-13}$	$1.3 \times 10^{-11}$	3%
$^{60}\text{Fe}/^{26}\text{Al}$	1.56	0.117	13.3

which, differently from C–O core AGB stars, ignite carbon in their cores prior to reaching the TP-AGB phase. The fate of these objects is unknown and they may end their lives as electron-capture SN or as massive ONe white dwarfs. First detailed nucleosynthetic predictions are currently being calculated (e.g., Pumo, 2007).

### 3. Comparison to data obtained from analysis of primitive meteorites

A currently much debated question regards the origin of short-lived radioactive nuclei, including  $^{26}\text{Al}$  and  $^{60}\text{Fe}$ , in the early solar system (see, e.g., Wasserburg et al., 2006). We could find a best fit solution for the observed abundances of  $^{26}\text{Al}$ ,  $^{41}\text{Ca}$ ,  $^{60}\text{Fe}$ , and  $^{107}\text{Pd}$  using the abundances predicted by our  $6.5 M_{\odot}$  AGB model and two free parameters: (i) the dilution factor of the AGB material into the material that collapsed to form our Sun, fixed to 330 parts of original material per 1 part of AGB material, and (ii) the time interval before the material was ejected by the AGB star and the formation of the first solid bodies in the proto-planetary disk, fixed to 0.53 Myr. This is the first time that an AGB star model provides a self-consistent solution for these four constraints. Our findings are discussed in detail in Trigo-Rodríguez et al., 2008.

Finally, meteoritic stellar grains from low-mass AGB stars typically show  $^{26}\text{Al}/^{27}\text{Al}$  ratios  $< 0.003$ . These can be explained by production of  $^{26}\text{Al}$  in the H-burning shell, however, the three orders of magnitude error bar of the  $^{26}\text{Al}(p, \gamma) ^{27}\text{Si}$  reaction does not allow a meaningful comparison between model predictions and observational data (van Raai et al., 2008). Grains showing  $^{26}\text{Al}/^{27}\text{Al}$  higher than 0.003 ratio may be explained by extra-mixing phenomena (Nollett et al., 2003) or may have formed from the last material to be expelled during the post-AGB star phase. This latter idea needs to be tested in detail.

### References

- Bao, Z.Y., Beer, H., Käppeler, F., Voss, F., Wisshak, K., Rauscher, T., 2000. *Atom. Data Nucl. Data Tables* 76, 70.
- Boothroyd, A.I., Sackmann, I.-J., Wasserburg, G.J., 1994. *ApJ* 430, L77.
- Frost, C.A., Lattanzio, J.C., 1996. *ApJ* 473, 383.
- Gallino, R. et al., 1998. *ApJ* 497, 388.
- García-Hernández, D.A. et al., 2007. *A&A* 462, 711.
- Herwig, F., 2005. *ARA&A* 43, 435.
- Izzard, R.G., Lugaro, M., Karakas, A.I., Iliadis, C., van Raai, M., 2007. *A&A* 466, 641.
- Karakas, A.I., Lattanzio, J.C., 2007. *PASA* 24, 103.
- Karakas, A.I., Lugaro, M., Wiescher, M., Goerres, J., Ugalde, C., 2006. *ApJ* 643, 471.
- Limongi, M., Chieffi, A., 2006. *ApJ* 647, 483.
- Lugaro, M. et al., 2004. *ApJ* 615, 934.
- Mowlavi, N., Meynet, G., 2000. *A&A* 361, 959.
- Nollett, K.M., Busso, M., Wasserburg, G.J., 2003. *ApJ* 582, 1036.
- Pumo, M.L., 2007. *MemSAIt* 78, 689.
- Trigo-Rodríguez, J.M., García-Hernández, A.D., Lugaro, M., Karakas, A.I., van Raai, M., García Lario, P., Manchado, A. 2008. *Meteorit. Planet. Sci.*, submitted for publication.
- van Raai, M.A., Lugaro, M., Karakas, A.I., Iliadis, C., 2008. *A&A* 478, 521.
- Ventura, P., D'Antona, F., 2005. *A&A* 431, 279.
- Wasserburg, G.J., Busso, M., Gallino, R., Nollett, K.M., 2006. *Nucl. Phys. A* 777, 5–69.